Editor's Choice

The Thermo-Economic Potential of ORC-Based Pumped-Thermal Electricity Storage: Insights from the Integrated Design of Processes and Working Fluids

Dominik Tillmanns, Dominik Pell, Johannes Schilling, and André Bardow*

Higher shares of renewable energy increase the need for electricity storage. A promising storage technology is Pumped-Thermal Electricity Storage (PTES): PTES systems transform electricity into heat using a heat pump (HP) and reconvert the heat into electricity using a heat engine. Since both HPs and heat engines require working fluids, maximum performance requires the optimal combination of PTES process and working fluids. Herein this work, the thermo-economic potential of an Organic Rankine Cycle (ORC)-based PTES system is analyzed by simultaneously designing both the PTES process and the working fluids used in the HP and the ORC. To rigorously explore the molecular design space, the 1-stage Continuous-Molecular Targeting - Computer-Aided Molecular Design method is employed. Detailed models for costing and sizing of the equipment allow for a thermo-economic design of the PTES. The computer-aided molecular design formulation integrates the working fluids as degrees of freedom into the process optimization. For the investigated ORC-based PTES system with an input power of 60 MW, the optimal process and working fluids minimize the specific investment cost to $\mathrm{SIC} = 929 \, € \, \mathrm{kWh}_{out}^{-1}$. The analysis of cost drivers shows that with decreasing compressor cost, the investigated ORC-based PTES system can become a competitive storage technology.

1. Introduction

In the last decade, the share of renewable energies in the energy system has increased in many parts of the world. As many renewable energy sources fluctuate, like wind and solar, a reliable energy supply requires a high capacity for electricity storage.[1] However, the established electricity storage technologies with high storage capacities have significant disadvantages: pumped-storage hydroelectricity (PSH) and compressed air energy storage (CAES) have low predicted specific costs but are geographically limited.[2] As alternative to PSH and CAES, large-scale battery-storage systems are predicted to have higher specific costs.[1] Additionally, battery-storage systems need specific materials like lithium for their production. Lithium is also needed for other applications such as electric cars or electric devices, leading to potential supply problems in the future without high recycling rates.[3] In addition to the established storage technologies, power-to-hydrogen-to-power (PtH$_2$tP) and power-to-methane-to-power (PtCH$_4$tP) have a promising outlook in the future, especially for long-term storage.[4] However, these technologies are not yet developed for large-scale electricity storage.

A promising alternative technology to store electricity is pumped-thermal electricity storage (PTES).[5] PTES systems use a heat pump (HP) to convert electric power into heat. The heat is then sent to a thermal-storage system. The stored thermal energy is reconverted into electric power using a heat engine (HE). PTES systems offer geographical flexibility as they have no geological restrictions.[6] Thereby, long electricity transport can be avoided. Furthermore, for the construction of PTES systems only abundant materials, like steel, are used.

The literature distinguishes three main types of PTES systems according to the HP and HE process used: Joule-based PTES systems,[7,8] transcritical PTES systems,[9,10] and Rankine-based PTES systems.[11–13] Joule-based PTES systems promise favorable round-trip efficiencies of around 70%.[7,8] However, these high system efficiencies rely on high-efficiency compressors and expanders such that Joule-based PTES systems have high specific investment cost (SIC) of up to 6000 \$ kW$_{el}^{-1}$.[14]

Transcritical PTES systems achieve round-trip efficiencies of up to 65%[9] with comparably low SIC of up to 2500 \$ kW$_{el}^{-1}$.[14]

D. Tillmanns, D. Pell, J. Schilling, A. Bardow
Chair of Technical Thermodynamics
RWTH Aachen University
Schinkelstraße 8, 52062 Aachen, Germany
E-mail: abardow@ethz.ch

J. Schilling, A. Bardow
Energy & Process Systems Engineering
Department of Mechanical and Process Engineering
ETH Zurich
Tannenstrasse 3, 8092 Zurich , Switzerland

A. Bardow
Institute of Energy and Climate Research–Energy Systems
Engineering (IEK-10)
Forschungszentrum Jülich GmbH
Wilhelm-Johnen-Straße, 52425 Jülich, Germany

The ORCID identification number(s) for the author(s) of this article can be found under https://doi.org/10.1002/ente.202200182.

However, transcritical PTES systems have low energy densities resulting in larger systems.[14] Thus, transcritical PTES systems are discussed for short-term storage with charge times below 10 h and discharge times below 5 h.[14] In contrast, Rankine-based PTES systems have comparably high energy densities and thus are discussed for charge and discharge times of up to 3 d.[14]

Rankine-based PTES systems can use a subcritical steam Rankine cycle[11] or a subcritical Organic Rankine Cycle (ORC)[12,13] as HE. Steam Rankine cycle-based PTES systems benefit from existing know-how on conventional power plants. Even more, existing conventional power plants could be converted for use as HEs in steam Rankine cycle-based PTES systems.[15] However, steam Rankine cycle-based PTES systems typically need thermal-storage systems with temperature levels up to 400 °C,[14] prohibiting the use of efficient vapor-compression HPs, which are only commercially available for temperatures up to 165 °C.[16]

In contrast, ORC-based PTES systems can exploit the broad experience with operating ORCs at temperatures up to 160 °C.[17] These systems can thus employ efficient, commercially available vapor-compression HPs to provide heat for the thermal-storage system. Additionally, ORC-based PTES systems have a high round-trip efficiency of up to 70% for idealized cycles and up to 55% for more realistic cycles shown by Roskosch and Atakan.[18] Furthermore, the design study of Roskosch and Atakan highlights that ORC-based PTES systems offer two fundamental degrees of freedom: first, process degrees of freedom such as pressure levels or mass flow rates can be optimized for the HP, the ORC, and the storage cycle. Second, the working fluids have to be selected for the HP and the ORC as well as the storage medium. Consequently, ORC-based PTES systems offer a high flexibility to tailor the systems to given specifications. Thus, in this work, we focus on ORC-based PTES systems.

A thermo-economically optimal ORC-based PTES system requires an optimal combination of processes and working fluids due to the strong interaction between processes and working fluids. However, so far, the thermo-economic potential of ORC-based PTES systems has only been analyzed for fixed, preselected working fluids,[19] leading to suboptimal solutions if the preselection fails.

Optimal combinations of working fluids and processes can be identified by integrating the molecule design into the process design.[20] For this purpose, computer-aided molecular design (CAMD) methods design molecular structures in silico. In CAMD methods, molecules are typically represented based on a discrete set of functional groups.[21] The design of molecules based on a set of functional groups allows capturing a wide range of molecular structures. However, the discrete molecular variables lead to a mixed-integer nonlinear programming (MINLP) problem (see the review of Papadopoulos et al.[20] for further information). A wide variety of solution methods have been developed solving the MINLP of integrated CAMD problems, for example, for working fluids in HPs,[22,23] and ORCs[24–32], as well as for solvents in liquid–liquid extraction[33–35] and absorption[36–42] and for reactions.[43,44] The integrated design methods mainly differ in the selected thermodynamic model, solution algorithm, or case study.[20,45]

In this work, we determine the thermo-economic potential of ORC-based PTES systems. For this purpose, we use the 1-stage Continuous-Molecular Targeting - Computer-Aided Molecular Design (CoMT–CAMD) method,[26,27] developed by some of the
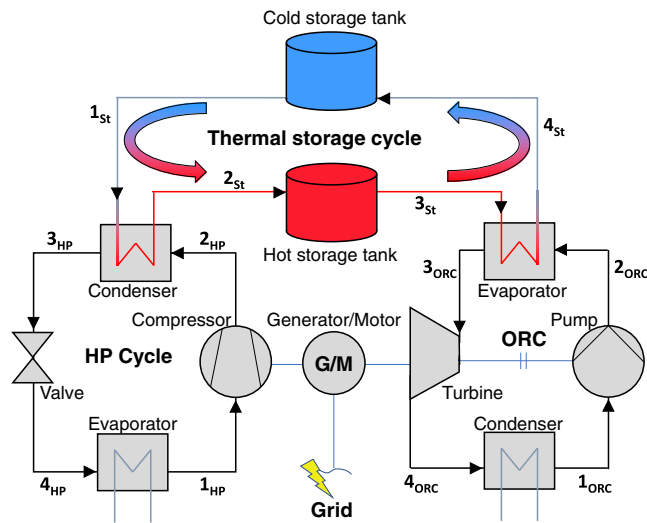
authors, to find an optimal combination of working fluids and processes for ORC-based PTES systems. The 1-stage CoMT–CAMD method enables the integrated thermo-economic design of molecules and processes based on a consistent thermodynamic model with strong predictive power, the perturbed-chain statistical associating fluid theory (PC-SAFT) equation of state (EoS).[46]

The paper is structured as follows: In Section 2, the ORC-based PTES system is described. Section 3 introduces 1-stage CoMT–CAMD for ORC-based PTES systems, including models for the process, equipment, and thermodynamics. The results of the integrated design of ORC-based PTES systems are presented, discussed, and compared to other electricity-storage technologies in Section 4. Finally, the main conclusions are drawn in Section 5.

2. ORC-Based PTES System

A basic ORC-based PTES system consists of three cycles (cf. **Figure 1**): an HP cycle, a thermal-storage cycle, and an ORC. During high renewable electric power production, the HP converts electrical energy into thermal energy, which is stored in a thermal-storage cycle. The stored thermal energy is reconverted using an ORC during low renewable electric power production. The heat-storage system is connected to the hot sides of the HP (condenser) and ORC (evaporator), as illustrated in Figure 1. In addition, a cold-storage system could be connected to the cold sides of the HP (evaporator) and ORC (condenser).[47] The studied basic configuration represents one of the three types of PTES systems in addition to Joule-based and transcritical PTES systems.[14]

In the following, the three cycles of a basic ORC-based PTES system with a heat-storage system are explained in detail: 1) In the HP cycle, a compressor increases the pressure of the working fluid vapor to the upper pressure level ($1_{HP} \rightarrow 2_{HP}$). The compressor is driven by an electric motor supplied by electrical energy from the grid. After compression, the superheated working fluid is condensed in the condenser by transferring heat to the thermal-storage cycle ($2_{HP} \rightarrow 3_{HP}$). After the condenser, a valve reduces the pressure of the liquid working fluid to the lower pressure level ($3_{HP} \rightarrow 4_{HP}$). To close the cycle, the working fluid is evaporated in the evaporator using heat from the environment ($4_{HP} \rightarrow 1_{HP}$). In the HP cycle, the degrees of freedom in an integrated design problem are the molecular structure of the working fluid and process variables (e.g., the pressure levels, the degree of subcooling in the condenser or the mass flow rate); 2) The thermal-storage cycle can use various cycle configurations (e.g., sensible or latent heat storage) and storage media (e.g., water or phase change materials). In this work, we focus on sensible heat storage using pressurized liquid water as the storage medium (cf. Figure 1) because this type of storage is environmentally friendly and cost-effective[47]. In the first step of the sensible heat-storage cycle, pressurized cold water from a cold-storage tank is heated in the condenser of the HP ($1_{St} \rightarrow 2_{St}$). Subsequently, the hot water is stored in a hot-storage tank for a certain period ($2_{St} \rightarrow 3_{St}$). Afterward, the hot water from the hot-storage tank is cooled in the ORC evaporator to evaporate the ORC working fluid ($3_{St} \rightarrow 4_{St}$). The cold water is then stored in the cold-storage tank to close the thermal-storage cycle ($4_{St} \rightarrow 1_{St}$). The degrees of freedom in the thermal-storage cycle are process variables like the mass flow rate to the hot- and

**ADVANCED
SCIENCE NEWS**

www.advancedsciencenews.com

Energy Technology
Generation, Conversion, Storage, Distribution

www.entechnol.de

Figure 1. Generic flow sheet of a basic Organic Rankine Cycle (ORC)-based pumped-thermal electricity storage (PTES) system with heat storage. The system includes an electric motor (M) to drive the heat pump (HP), thermal storage (St), and an ORC driving a generator (G).

the cold-storage tank, the temperature level in the hot- and the cold-storage tank or the geometrical parameters of the storage tanks; and 3) In the ORC, the pressure of the liquid working fluid is increased to the upper pressure level by a pump ($1_{ORC} \rightarrow 2_{ORC}$). After the pump, the working fluid is evaporated in the evaporator by the heat of the hot-storage medium ($2_{ORC} \rightarrow 3_{ORC}$). The evaporated working fluid is then expanded

in the turbine to generate mechanical power, which is transferred to electrical power by a generator ($3_{ORC} \rightarrow 4_{ORC}$). To close the cycle, the expanded working fluid is condensed in the condenser using the environment as the heat sink ($4_{ORC} \rightarrow 1_{ORC}$). In the ORC, the degrees of freedom of an integrated design problem are similar to the HP: the molecular structure of the working fluid and process variables (e.g., the pressure levels, the degree of superheating in the evaporator or the mass flow rate).

In this work, the basic ORC-based PTES system configuration is considered. In general, the cycle configuration of the three primary cycles is a further degree of freedom of the PTES system.[15] For example, an additional heat exchanger for internal heat recovery can improve the efficiency of the ORC.[48] However, at the same time, the additional heat exchanger increases the investment costs and can thus be economically less efficient.[49] The cycle configuration can be considered as a degree of freedom of the integrated design problem by a superstructure-based design in future work.[49]

3. Design of Basic ORC-Based PTES Systems Using 1-Stage CoMT–CAMD

To identify thermo-economically optimal ORC-based PTES systems, we optimize processes and working fluids in the integrated design method 1-stage CoMT–CAMD.[26,27] The general MINLP problem formulation of 1-stage CoMT–CAMD is given for ORC-based PTES systems in Problem (1):

$$
\begin{aligned}
&\min_{x,\, y^S_{HP/ORC}} && f\left(x, \theta_{HP/ORC}, \kappa_{HP/ORC}\right) && \text{objective} \\[4pt]
&\text{s.t.} && g_1\left(x, \theta_{HP/ORC}, \kappa_{HP/ORC}\right) \le 0 && \left.\begin{array}{l}\text{equipment sizing for HP,}\\ \text{storage cycle and ORC}\end{array}\right\} \\
& && g_2\left(x, \theta_{HP/ORC}, \kappa_{HP/ORC}\right) = 0 && \\[4pt]
& && \kappa_{HP/ORC} = k\left(x, \theta_{HP/ORC}, y^S_{HP/ORC}\right) && \text{PC-SAFT(transport)} \\[4pt]
& && p_1\left(x, \theta_{HP/ORC}\right) \le 0 && \left.\begin{array}{l}\text{process model for HP,}\\ \text{storage cycle and ORC}\end{array}\right\} \\
& && p_2\left(x, \theta_{HP/ORC}\right) = 0 && \\[4pt]
& && \theta_{HP/ORC} = h\left(x, y^S_{HP/ORC}\right) && \text{PC-SAFT(equilibrium)} \\[4pt]
& && F_1 \cdot y^S_{HP/ORC} = d && \left.\begin{array}{l}\text{CAMD model for HP and}\\ \text{ORC working fluid}\end{array}\right\} \\
& && F_2 \cdot y^S_{HP/ORC} \le d && \\[4pt]
& && x_{lb} \le x \le x_{ub} \in \mathbb{R}^n && \\
& && y^S_{lb,HP/ORC} \le y^S_{HP/ORC} \le y^S_{ub,HP/ORC} \in \mathbb{Z}^l &&
\end{aligned}
\tag{1}
$$

In Problem (1), f is the objective function to be optimized. In this work, we consider the SIC more specific (SIC_{out}) as the thermo-economic objective function calculated as the total capital investment ($I_{0,tot}$) per electrical output capacity ($P_{out} \cdot t_{discharge}$)

$$
SIC_{out} = \frac{I_{0,tot}}{P_{out} \cdot t_{discharge}}
\tag{2}
$$

This objective function captures the trade-off between investment and round-trip efficiency of the PTES system. Thereby, the

objective function enables comparing the results to storage technologies with different efficiencies (see Section 4.4). The advantage of the SIC compared to other alternative economic objective functions, like the net present value, is that no assumptions are required regarding the location-dependent interest rate or electricity prices during charging and discharging. The SIC_{out} depends on the process degrees of freedom x, both the equilibrium properties θ_{HP} and θ_{ORC} and the transport properties κ_{HP} and κ_{ORC} of the working fluids in HP and ORC. The process degrees of freedom $x = (x_{HP}, x_{St}, x_{ORC})^T$ are composed of the

**ADVANCED
SCIENCE NEWS**

www.advancedsciencenews.com

Energy Technology
Generation, Conversion, Storage, Distribution

www.entechnol.de

degrees of freedom of the HP x_{HP} (e.g., the degree of subcooling in the condenser or the mass flow rate), storage cycle x_{St} (e.g., the temperature level in the hot- and the cold-storage tank), and ORC x_{ORC} (e.g., the degree of superheating in the evaporator or the pressure levels). The equipment and process models consist of inequality constraints g_1 and p_1 (e.g., turbine limitations or limits of the minimal approach temperature) as well as equality constraints g_2 and p_2 (e.g., heat-transfer correlations or energy balances) (for details, see Sections 3.1 and 4.1). The equilibrium properties θ and the transport properties κ of the ORC and HP working fluids are calculated using the PC-SAFT equation of state[46] as thermodynamic model (see Section 3.2 for details). The working fluids of the ORC and HP are represented by integer vectors γ_{ORC}^S and γ_{HP}^S, respectively. The integer vectors indicate the number of functional groups constituting the molecular structure of the working fluids. The molecular structures are designed as degree of freedom of the optimization using a CAMD formulation. The CAMD formulation ensures structural feasibility of the molecular structures γ_{ORC}^S and γ_{HP}^S by equality constraints F_1 and inequality constraints F_2 (e.g., the octet rule).[50–52]

The integrated design problem is modeled using the gPROMS ProcessBuilder v1.2.[53] To solve the integrated design problem in Problem (1), we use the local solver OAERAP (Outer Approximation Equality Relaxation Augmented Penalty) available in gPROMS ProcessBuilder v1.2. The OAERAP solver splits the MINLP problem into a series of nonlinear program (NLP) subproblems and mixed-integer linear program (MILP) master problems. The first NLP relaxes the discrete degrees of freedom in Problem (1) resulting from the integer values of the molecular structures. Thus, the relaxation problem does not yield real molecular structures. However, the result can be regarded as hypothetical, optimal working fluids for HP and ORC, the so-called target, representing a lower bound for the objective function. Subsequentially, an optimal integer solution is identified using outer-approximation.[54] The result of the MINLP is an optimal working fluid pair jointly with the corresponding optimal process variables and equipment sizes for all cycles. To obtain a ranking of the best working fluid pairs, the MINLP can be solved repeatedly, prohibiting all already found solutions using integer-cut constraints.[55] A ranking of the best working fluid pairs helps to avoid local optima identified by the local solver and considering nonconventional fluid properties a posteriori, which are not captured in the thermodynamic model.

In Section 3.1, the thermo-economic process and equipment model is described in detail and the thermodynamic model is introduced in Section 3.2.

3.1. Thermo-Economic Process and Equipment Model of the PTES

In this work, we investigate the potential of a subcritical, basic ORC-based PTES system for large-scale electricity storage using a quasi-steady-state model. To obtain the total capital investment $I_{0,tot}$ of the basic ORC-based PTES system, the equipment is designed and the purchased-equipment cost $I_{0,i}$ is calculated for each equipment i. The cost for construction, piping, transport, control electronics, real estate, buildings, and planning

is considered by an additional factor of 3.4 to calculate the total capital investment $I_{0,tot}$ of the basic ORC-based PTES system[56]

$$I_{0,tot} = 3.4 \cdot \sum_{i \in I} I_{0,i} \tag{3}$$

For each cycle, mass and energy balances are implemented. The turbomachinery is assumed to be adiabatic with constant isentropic efficiencies. Two additional design constraints are considered for the turbine to avoid high Mach numbers and large blade heights. For the turbine, a fluid-dependent cost correlation is used to calculate the purchased-equipment cost.[57] In contrast, fluid-independent cost correlations are used for the pump[58] and the compressor,[59] calculating the purchased-equipment cost from the power input. For the compressor, the used cost correlation for radial compressors is limited to a power input of 30 MW.[59] Thus, in case of an input power of the PTES higher than 30 MW, we consider several compressors with a maximal compressor power of 30 MW each. The purchased-equipment cost of the generator is calculated from the power output of the generator.[57] The purchased-equipment cost of the gearbox is calculated from the purchased-equipment cost of the generator.[57]

The heat exchangers are modeled as counter-flow shell-and-tube heat exchangers without pressure losses. The required heat exchanger area is calculated using detailed heat-transfer correlations for single-phase heat transfer,[60] flow boiling,[61] and film-wise condensation.[62] The correlations for flow boiling and filmwise condensation depend on the steam quality and thus describe the local heat transfer. Therefore, we discretize the evaporators and condensers and calculate the heat exchanger area for each discrete element using a mean steam quality. The discretized areas are summed to calculate the total heat exchanger area. The purchased-equipment costs of the heat exchangers are calculated from the heat exchanger areas using a cost correlation from Smith.[56] The valve in the HP cycle is assumed to be adiabatic and its purchased-equipment cost is assumed to be negligible since the valve is a low-cost component.[10] The detailed thermodynamic models of the HP and ORC process and models for equipment sizing are given in Supporting Information SI A 1. The calculation of the investment costs for the HP and ORC equipment is provided in Supporting Information SI A 2.

As storage medium, we use liquid water, which is optionally pressurized. The hot- and cold-storage tanks are assumed to be adiabatic due to the short storage time in the investigated daily storage case study. Pressure losses in the storage cycle are neglected. The storage tanks are sized based on two norms, DIN EN 13 455-3[63] and EN 14 015:2004.[64] Following the norms, the storage tanks are sized depending on the storage pressure, storage temperature, and mass of the storage medium in the tanks. A foundation and thermal isolation are considered for the tanks to justify the assumption of adiabatic storage tanks. The purchased-equipment costs of the storage tanks are calculated using a detailed cost correlation from Jacob et al.[65] The design of the storage tanks is explained in detail in Supporting Information SI A 3.

An overview of all sizing models and cost correlations is given in **Table 1** and **2**, respectively.

ADVANCED
SCIENCE NEWS
www.advancedsciencenews.com

Energy Technology
Generation, Conversion, Storage, Distribution

www.entechnol.de

Table 1. Overview of the design approaches and the main features used in this work.

Equipment	Design approach	Reference	Features
Compressor	Isentropic efficiency	[66]	
	Single-phase heat transfer	[60]	
Heat exchanger	Evaporation	[61]	Discretized, iterative
	Condensation	[62]	Discretized
Storage tank	Detailed design method	[63,64]	Pressure-dependent
Pump	Isentropic efficiency	[66]	
Turbine	Isentropic efficiency	[66]	
	Design constraints	[57]	Fluid-dependent

Table 2. Overview of the cost correlations and their main input parameter(s) used in this work.

Equipment	Cost correlation from	Input
Compressor	Towler and Sinnott[59]	Compressor power
Heat exchanger	Smith[56]	Heat exchanger area
Storage tanks	Jacob et al.[65]	Various parameters
Pump	Turton et al.[58]	Pump power
Turbine	Astolfi et al.[57]	Number of stages, size parameter
Generator	Astolfi et al.[57]	Turbine power output
Gearbox	Astolfi et al.[57]	Generator costs

3.2. Thermodynamic Model

Our method for the integrated thermo-economic design of processes and working fluids uses the PC-SAFT[46] equation of state (EoS) to calculate both equilibrium θ and transport properties κ of the working fluids. In PC-SAFT, a molecule is modeled as perturbed chains of spherical segments, which are represented by typically three to seven physically based pure component parameters z. In this work, we consider only nonassociative and nonpolar working fluids. Consequently, three pure component parameters are sufficient to describe a working fluid: the segment number m and the segment diameter σ to represent the geometry of the chains and the segment dispersion energy ε/k to describe the van der Waals attraction.

To link PC-SAFT to the CAMD formulation, the pure component parameters of PC-SAFT are calculated from the molecular structure of the working fluids using the homosegmented group contribution (GC) method of PC-SAFT.[67] In this method, the pure component parameters z are calculated from the molecular structure of the working fluid γ^S using the mixing rule of Vijande et al.[68]

$$m = \sum_{k \in K} n_k \cdot m_k \tag{4}$$

$$m \cdot \sigma^3 = \sum_{k \in K} n_k \cdot m_k \cdot \sigma_k^3 \tag{5}$$

$$m \cdot \varepsilon/k = \sum_{k \in K} n_k \cdot m_k \cdot (\varepsilon/k)_k \tag{6}$$

where n_k represents the number of functional groups of type k in the molecular structure. These values constitute the molecular structure vector γ^S. The parameters m_k, σ_k, and $(\varepsilon/k)_k$ indicate the contributions of the functional group of type k to the pure component parameters.

Since PC-SAFT is based on the residual Helmholtz energy, a reference property is needed to calculate absolute thermodynamic properties. In this work, the reference property is the heat capacity of the ideal gas c_p^{ig}. We calculate the heat capacity of the ideal gas c_p^{ig} from the molecular structure of the working fluids $\gamma^S_{ORC/HP}$ using Joback's GC method.[69]

The transport properties κ are calculated from PC-SAFT using the GC methods proposed by Lötgering-Lin and Gross[70] for viscosities η and by Hopp and Gross[71] for thermal conductivities λ. Both methods are based on Rosenfeld's entropy scaling.[72,73] In these methods, the transport properties are calculated as product of a reduced and a reference transport property. The reduced transport properties are calculated using univariate functions of the residual entropy. The reference properties are calculated based on the Chapman–Enskog viscosity and the Chapman–Enskog thermal conductivity.

In this work, we consider the following set of functional groups: $-CH3$, $-CH2-$, $>CH-$, and $>C<$ for branched alkanes and $=CH2$, $=CH-$, and $>C=$ for branched alkenes. The set of functional groups is limited since we require GC methods for both the PC-SAFT parameters and the transport properties. In particular, data on transport properties is scarce such that the development of GC methods is restricted.[71] In this work, we are further limited to nonpolar functional groups since the polar interactions of PC-SAFT[74,75] are not implemented in gPROMS ProcessBuilder v1.2. Moreover, the integrated design problem in Problem (1) is challenging, limiting the number of integer degrees of freedom to ensure a robust and reliable convergence of the MINLP solver. In general, additional functional groups can be easily integrated into the integrated design method as soon as new functional groups are fitted to measurement data, polar interactions of PC-SAFT are considered in gPROMS ProcessBuilder or more powerful MINLP solvers are available. Nevertheless, the molecular design space considered in this work is reasonable since alkanes and alkenes are essential working fluids for ORCs and HPs.

4. Results and Discussion

The 1-stage CoMT–CAMD method is used for the integrated thermo-economic design of an ORC-based PTES system for the case study presented in Section 4.1. The results of the integrated design are discussed in Section 4.2. An uncertainty analysis for the cost correlation of the main cost contributor is carried out in Section 4.3. In Section 4.4, we compare the thermo-economically optimal ORC-based PTES system with alternative electricity storage technologies.

4.1. Case Study

As case study, we consider a large-scale PTES system for daily storage based on Henchoz et al.[66] The constant power input

**ADVANCED
SCIENCE NEWS**
www.advancedsciencenews.com

Energy Technology
Generation, Conversion, Storage, Distribution
www.entechnol.de

Table 3. Specifications of the ORC-based PTES system based on Henchoz et al.[66]

Parameter	Symbol	Value
Compressor power input	$P_{el, in}$	60 MW
Isentropic compressor efficiency	$\eta_{C, is}$	0.88
Isentropic turbine efficiency	$\eta_{T, is}$	0.9
Isentropic pump efficiency	$\eta_{P, is}$	0.85
Min. absolute pressure (HP/ORC)	$p_{min, HP/ORC}$	1 bar
Max. absolute pressure (HP/ORC)	$p_{max, HP/ORC}$	60 bar
Min. absolute pressure (storage)	$p_{min, storage}$	1 bar
Max. absolute pressure (storage)	$p_{max, storage}$	5 bar
Max. charge time	$t_{max, charge}$	8 h
Max. overall cycle time	$t_{max, tot}$	24 h

of $P_{el, in} = 60\,MW$ is available for up to 8 h (cf., **Table 3**), whereby the charge time t_{charge} can be optimized between 1 and 8 h. The constant discharge power $P_{el, out}$ is a process degree of freedom. The overall cycle time for charging and discharging $t_{tot} = t_{charge} + t_{discharge}$ is limited to 24 h as a constraint in the optimization to ensure a daily storage cycle. The total energy stored during the charge time has to be discharged within the overall cycle time, ensuring the PTES system's cyclic operation. A typical charge–discharge trajectory is shown in **Figure 2** for an ORC-based PTES system using propane in the ORC and isobutene in the HP from the case study.

The minimal approach temperature in all heat exchangers is set to 2 K since smaller values increase cost strongly, impacting optimization stability. The inlet temperature of the cooling water in the HP evaporator and ORC condenser is assumed to be $T_{CW, in} = 10\,°C$.[76]

It should be noted that the case study chosen in this work is just one example of the broad application range of PTES systems, which can strongly vary, for example, in power input, capacity, or cycle time.[14] The SIC is expected to be substantially influenced by the case study. Typically, a higher power input results in a larger PTES system with more electrical output capacity. Since the equipment used in PTES systems follows the rules of economy of scale, PTES systems with a higher power input are expected to result in lower SIC per electrical output capacity. Longer overall cycle times have been shown to reduce SIC per electrical output capacity.[14] The impact of the case study specification on the identified optimal working fluids should thus be analyzed in future work.

The degrees of freedom of the integrated design of the ORC-based PTES system given in Problem (1) are the process variables x as well as the molecular structure of the working fluids in the ORC y_{ORC}^S and in the HP y_{HP}^S. In the HP, we consider the following process variables as degrees of freedom: 1) the mass flow rate of the HP working fluid $\dot{m}_{HP}$; 2) the degree of subcooling at the HP condenser outlet ΔT_{sc}; 3) the degree of superheating at the HP evaporator outlet $\Delta T_{sh, HP}$; and 4) the pressure level at the outlet of the HP valve $p_{low, HP}$.

These degrees of freedom are typical design parameters in a thermodynamic model of an HP cycle.[77] In general, the upper pressure level of the HP cycle can also be a process degree of freedom. However, in our case study, we assume a fixed, predefined power input of the compressor (cf., Section 4.1). In this case, the upper pressure level of the HP cycle is not a degree of freedom but calculated from the thermodynamic compressor model.

In the thermal-storage cycle with the predefined storage medium water (cf., Section 2), the process degrees of freedom considered in this work are: 1) the mass flow rate to charge the hot-storage tank $\dot{m}_{charge}$; 2) the mass flow rate to discharge the hot-storage tank $\dot{m}_{discharge}$; 3) the charge time t_{charge}; 4) the pressure in the storage cycle $p_{storage}$; 4) the temperature in the cold-storage tank $T_{storage, cold}$; and 5) the height-to-diameter ratio of the storage tanks $(H/d)_{tank, hot/cold}$.

The mass flow rates for charging and discharging as well as the temperature in the cold-storage tank are chosen as degrees of freedom to optimally link the thermal-storage cycle to the HP cycle and the ORC. The charge time is a degree of freedom in this work because the thermal-storage cycle is not modeled as
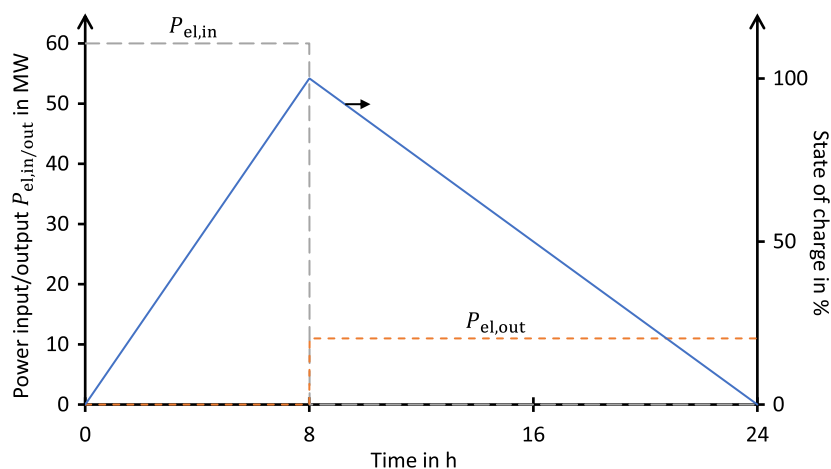
Figure 2. The power input $P_{el, in}$, power output $P_{el, out}$, and the state of charge of the storage tanks exemplified for an ORC-based PTES system using propane in the ORC and isobutene in the HP.

**ADVANCED
SCIENCE NEWS**

www.advancedsciencenews.com

Energy Technology
Generation, Conversion, Storage, Distribution

www.entechnol.de

a closed cycle to improve convergence. Instead, the state at the outlet of the cold-storage tank is related to the inlet of the HP condenser by adding a constraint. The pressure in the thermal-storage cycle is essential to ensure the liquid state of the water. The height-to-diameter ratio of the storage tanks is an important design parameter determining the size of the storage tanks and the corresponding material cost (cf., Supporting Information SI A 3).

In the ORC, we consider the following process variables as the degrees of freedom: 1) the mass flow rate of the ORC working fluid $\dot{m}_{ORC}$; 2) the pressure level at the outlet of the ORC pump $p_{high, ORC}$; 3) the power output of the ORC turbine $P_{ORC, out}$; 4) the number of turbine stages n_{St}; and 5) the degree of superheating at the ORC evaporator outlet $\Delta T_{sh, ORC}$.

These degrees of freedom are often used design parameters for ORCs.[25–27] We choose the power output of the ORC turbine as a degree of freedom instead of the commonly used pressure level at the outlet of the ORC turbine due to convergence reasons.

In summary, Problem (1) has 15 continuous process degrees of freedom, 40 binary degrees of freedom representing the working fluids, and 1 integer process degree of freedom.

4.2. Results of the Integrated Thermo-Economic Design of ORC-Based PTES Systems

We perform the integrated, thermo-economic design considering the SIC_{out} as the objective function (Equation (2)). Initially, the relaxation problem is solved in 1-stage CoMT–CAMD. The result of the relaxation problem is a hypothetical, optimal working fluid pair of HP and ORC with SIC = 914 € kWh$_{out}^{-1}$ and a round-trip efficiency of $\eta = 37.2\%$ (**Table 4**), where the round-trip efficiency is defined as

$$\eta = \frac{P_{el, out} \cdot t_{discharge}}{P_{el, in} \cdot t_{charge}} \quad (7)$$

The objective function value of this so-called target represents a lower bound for the SIC. The best identified real working fluid pair for the considered basic ORC-based PTES system is propane for the ORC and isobutene for the HP with $SIC_{out} = 929$ € kWh$_{out}^{-1}$ and $\eta = 36.7\%$ (Table 4).

Thus, the SIC of the best real working fluid pair is only 1.6% higher than the SIC of the target showing the small room for further improvement within the considered molecular design

Table 4. The target and the top 5 working fluid pairs for an ORC-based PTES system identified by a thermo-economic optimization using 1-stage CoMT–CAMD, the specific investment cost (SIC_{out}) in € kWh$_{out}^{-1}$ (objective function) and the round-trip efficiency η in %.

Ranking	ORC working fluid	HP working fluid	SIC_{out} in € kWh$_{out}^{-1}$	η in %
–	Target	Target	914	37.2
1	Propane	Isobutene	929	36.7
2	Propane	1-Butene	934	36.4
3	Propene	Isobutene	952	34.5
4	Propane	2-Butene	952	38.0
5	Propene	1-Butene	957	34.3

space. However, it should be noted that the target value strongly depends on the molecular design space. The consideration of further molecule classes could reduce the cost of the considered ORC-based PTES system.

A ranking of the top five real working fluid pairs is calculated (see Table 4). The average computational time to find an optimal working fluid pair is 24 min. Consequently, a ranking of the top five working fluid pairs is obtained in approximately 2 h. In the top five, a C3 alkane or alkene is identified as working fluid for the ORC and a C4 alkene for the HP. For the considered subcritical HP and ORC cycles, the critical temperature of the working fluids is important. The C4 alkenes have higher critical temperatures than C3 alkanes/alkenes and, thus, enable higher temperature levels in the HP. Since the HP cycle needs a higher temperature level than the ORC to transfer heat to the storage medium (cf. **Figure 3**), working fluids with higher critical temperatures are preferred in the HP cycle. The temperature–enthalpy diagram shows that both the HP compressors and the ORC turbine potentially enter the two-phase region. Thus, the potential formation of liquid droplets should be checked in further studies.
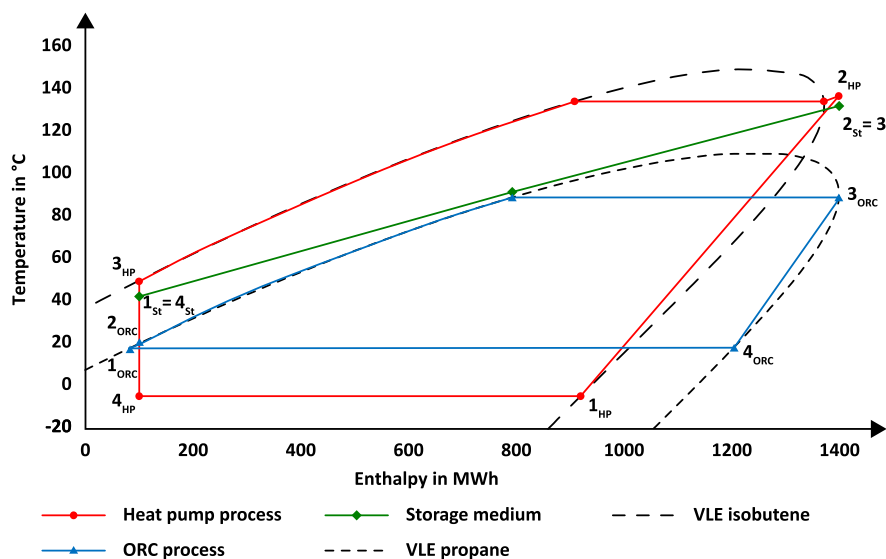
However, 1-butene[13,19] and propene[19] are also discussed as possible working fluids for the HP cycle and ORC for similar ORC-based PTES systems in the literature. In these PTES systems, the same working fluid is considered for both the HP cycle and the ORC. In the present work, the integrated design of the ORC-based PTES system demonstrates that different working fluids in the HP and the ORC can improve the thermo-economic performance of the process.

In our top five, the SIC is correlated to the round-trip efficiency η. However, the fourth-ranked working fluid pair propane/2-butene is an outlier to that correlation highlighting the difference between a thermodynamic and thermo-economic objective function. To further analyze this difference, an integrated thermodynamic design is carried out using the round-trip efficiency η as objective function for the same case study (see Supporting Information SI B). The thermodynamic design leads to similar top five working fluid pairs and the same optimal working fluid pair propane/isobutene as in the thermo-economic design. The thermodynamic design improves the round-trip efficiencies by approximately 5–6 percentage points for the top five working fluid pairs compared to the thermo-economic design. At the same time, the SIC is increased by up to 173% (for more details, see Supporting Information SI B).

To further analyze the composition of the SIC_{out}, **Figure 4** shows the cost distribution for the best working fluid pair in the thermo-economic design.

The HP equipment is considerably more expensive (71% of the total capital investment) than the ORC equipment (22%). The storage cycle is the cheapest primary cycle and requires only 7% of the total capital investment. In the HP cycle, larger and thus more expensive equipment is needed due to the high power input ($P_{el, in} = 60$ MW) and the shorter charge time (8 h). In contrast, the ORC equipment is smaller due to a lower power output of the ORC ($P_{el, out} = 11$ MW) and a longer discharge time (16 h) reducing mass flows almost by half (see **Table 5**).

For the best working fluid pair propane/isobutene, a high degree of subcooling (85 K) in the condenser of the HP is

ADVANCED
SCIENCE NEWS

www.advancedsciencenews.com

Energy Technology
Generation, Conversion, Storage, Distribution

www.entechnol.de

Figure 3. Temperature–enthalpy diagram for the thermo-economically optimal ORC-based PTES system using propane for the ORC and isobutene for the heat pump.
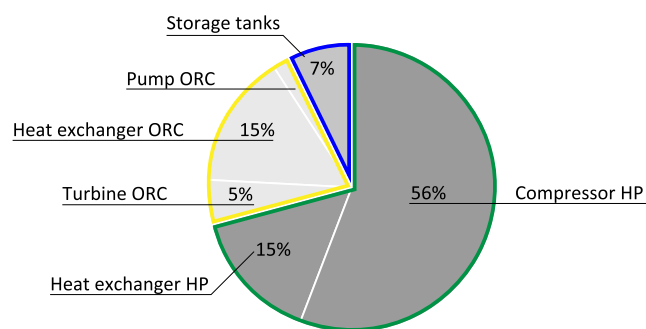
Figure 4. Cost distribution of the total capital investment of the thermo-economically optimal ORC-based-PTES system using propane in the ORC and isobutene in the HP. Dark grey represents the HP costs, medium grey the storage cycle costs, and light grey the ORC costs.

favorable. This high degree of subcooling results in better matching temperature profiles of the HP working fluid and the sensible storage medium (cf. Figure 3). Thereby, exergy losses are minimized during heat transfer. In contrast, superheating after evaporation is not favorable for both the HP and the ORC due to the small heat capacities of the working fluid vapors and the resulting small economic potential. The optimal hot-storage temperature is $T_{high} = 130\,°C$ and the optimal cold-storage temperature is $T_{low} = 43\,°C$. For these storage temperatures, the minimal approach temperature of 2 K is reached (cf. Figure 3) leading to an optimal match between the temperature profiles of the HP working fluid in the condenser, the sensible storage medium, and the ORC working fluid in the evaporator. The maximal charge time of 8 h (upper bound) is favorable because the maximal amount of energy can be stored and reconverted. Furthermore, except for the purchased-equipment cost of the storage, most of the purchased-equipment cost $I_{0,i}$ depends on the power input or output of the equipment. In particular, the

Table 5. Process variables for the thermo-economically optimal ORC-based PTES system using propane in the ORC and isobutene in the HP. Bold variables represent optimization degrees of freedom and the asterisk marks variable values at their bound. For easier readability, we rounded all values to two significant digits.

ORC			Heat pump			Storage		
Working fluid: Propane			**Working fluid**: Isobutene			Storage medium: Water		
Variable	Value	Unit	Variable	Value	Unit	Variable	Value	Unit
$\dot{m}_{ORC}$	200	kg s^{-1}	$\dot{m}_{HP}$	380	kg s^{-1}	$\dot{m}_{charge}$	430	kg s^{-1}
$p_{high,ORC}$	35	bar	$p_{high,HP}$	33	bar	$\dot{m}_{discharge}$	220	kg s^{-1}
$p_{low,ORC}$	7.8	bar	$\boldsymbol{p_{low,HP}}$	1.0	bar	$T_{storage,\,cold}$	43	°C
$\Delta T_{sh,ORC}$	0*	K	$\Delta T_{sh,HP}$	0*	K	$T_{storage,\,hot}$	130	°C
			ΔT_{sc}	85	K	$\boldsymbol{p_{storage}}$	3.1	bar
						$\boldsymbol{t_{charge}}$	8*	h
						$\boldsymbol{t_{discharge}}$	16*	h
						$Q_{storage}$	1300	MWh

main cost contributor, the compressor (cf. Figure 4), has purchased-equipment cost that is independent of the process variables and working fluids in the investigated case study (cf. Section 4.1) since a constant power input is assumed. Consequently, the maximal charge time reduces SIC per electrical output capacity due to a significantly higher electrical output capacity and only slightly higher total capital investment. Similarly, a maximal discharge time of 16 h, which is the upper bound for a charge time of 8 h, is favorable because the mass flow rate in the ORC is reduced, resulting in smaller and less expensive ORC equipment. The optimal process variables for the best working fluid pair propane/isobutene identified by a thermodynamic optimization are shown and discussed in Supporting Information SI B.

### 4.3. Uncertainty Analysis of the Compressor Cost Correlation

The compressors in the HP contribute most to the total capital investment (cf. Section 4.2). Consequently, the compressor cost is most important to reduce PTES system cost. Furthermore, an accurate prediction of the compressor cost is essential to achieve reliable results. In this work, we select two compressors with 30 MW nominal power each because the cost correlation used for the radial compressor is limited to 30 MW (see Section 3.1). Thus, we can expect benefits from dedicated larger compressors. However, large-scale compressor systems are rarely investigated in the literature and, consequently, no suitable correlation was found for the purchased-equipment cost of large-scale compressor systems. Thus, the cost correlation for the compressor is expected to introduce the largest inaccuracies to the model. Consequently, these inaccuracies are analyzed.

To quantify the uncertainties of the cost correlation for the compressor, we compare the SIC considering two additional cost correlations for the compressor. For this purpose, the integrated design with 1-stage CoMT–CAMD is repeated using the cost correlations for compressors of Seider et al.[78] and Henchoz et al.[66] Both correlations calculate the purchased-equipment cost for radial compressors from the power input $I_{0,C} = f(P_{el,in})$. As no upper limit for the range of applications is given in both references, we chose the same limit as for the correlation of Towler and Sinnott[59] (30 MW) for a better comparison. As a result, the SIC of the optimized PTES system varies from $542 \ €\,kWh_{out}^{-1}$ for the compressor cost correlation from Henchoz et al.[66] to $1215 \ €\,kWh_{out}^{-1}$ for the compressor cost correlation from Seider et al.[78] Compared to the previous result calculated using the cost correlation from Towler and Sinnott, the SIC deviates by -42% and $+31\%$, respectively. Thus, the chosen compressor cost correlation has a high impact on the predicted SIC of PTES systems. The comparison underlines the need for an accurate cost correlation for large-scale compressors. More research is needed in the future to quantify the purchased-equipment cost of large-scale compressors reliably. We use the uncertainties of the compressor cost correlation for the following comparison with alternative electricity-storage technologies.

4.4. Comparison of PTES Systems with Alternative Electricity-Storage Technologies

To quantify the economic potential of ORC-based PTES systems, we compare the PTES system to alternative electricity-storage technologies. For this purpose, the results from Section 4.2 are compared to the SIC of other electricity storage technologies with high storage capacities for today and 2030 (see **Figure 5**). The data used to calculate the SIC of the technologies are taken from the literature (**Table 6**).

The SIC for PSH is expected not to change from today to 2030 because the underlying cycles are based on established technologies and no major additional learning effects are expected.[81] Thus, we assume the same SIC in 2030 as for today, which is a conservative assumption. All costs are converted to SIC per electrical output capacity in $€\,kWh_{out}^{-1}$. For a better comparison, we use the optimal ORC-based PTES system (cf. Section 4.2) as a reference system in terms of power output (in kW_{el}) and
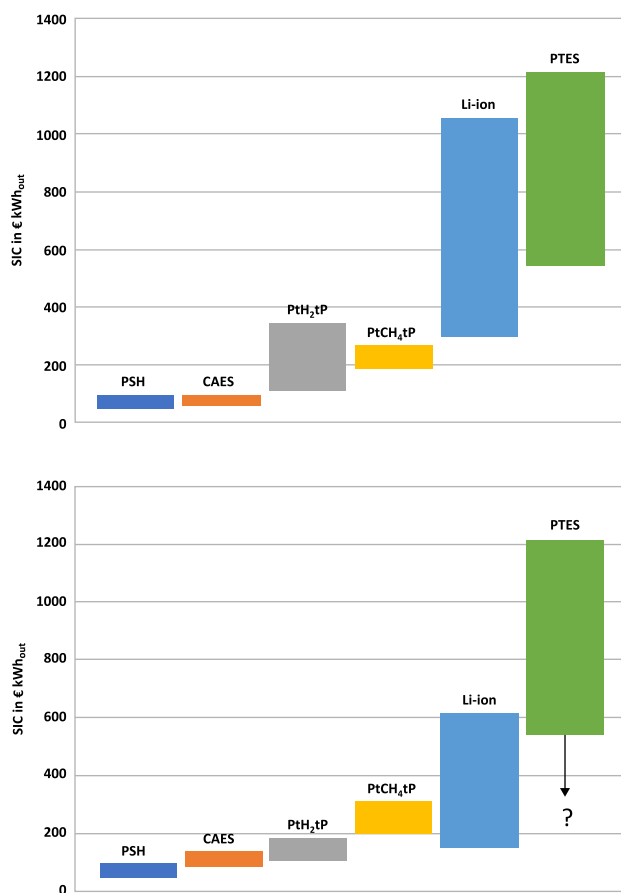
Figure 5. Comparison of the SIC in $€\,kWh_{out}^{-1}$ today (top) and in 2030 (bottom) for the optimal ORC-based PTES systems using three cost correlations for the compressor purchased-equipment cost[59,66,78] with pumped-storage hydroelectricity (PSH), compressed air energy storage (CAES), Li-ion batteries (Li-ion), power-to-hydrogen-to-power (PtH$_2$tP), and power-to-methane-to-power (PtCH$_4$tP). An overview of the sources for the SIC is given in Table 6. All costs are converted to SIC in $€\,kWh_{out}^{-1}$ using the optimal ORC-based PTES system as a reference system in terms of power output (in kW_{el}) and electrical energy output capacity (in kWh_{out}) of the storage systems (see Supporting Information SI C for details). The question mark indicates a possible trend for the costs of ORC-based PTES systems until 2030, which is not captured in this work.

electrical energy output capacity (in kWh_{out}) of the storage systems. The assumptions and conversions are described in detail in Supporting Information SI C. For the identified ORC-based PTES system, the given range of the SIC is the range of the optimization results using the three considered cost correlations for the compressor purchased-equipment cost (cf. Section 4.3).

Please note that the SIC chosen for comparison is only one potential economic performance indicator. To compare possible business cases for storage technologies in detail, further economic performance indicators should be considered, for example, the net present value. The net present value would need location-dependent assumptions regarding the interest rate and electricity prices during charging and discharging. Thus, our comparison based on the SIC depends less on location. The SIC thus indicates a more general economic competitiveness.[82]

Table 6. Overview of the sources for the specific investment cost of electricity-storage technologies with high-storage capacities for today and 2030.

Technology	Reference for today	Reference for 2030
Pumped-storage hydroelectricity (PSH)	Jülch[4]	Same as calculated for today
Compressed air energy storage (CAES)	Jülch[4]	Jülch[4]
Li-ion batteries (Li-ion)	Upper bound: Jülch[4]	Upper bound: Jülch[4]
	Lower bound: Breyer et al.[79]	Lower bound: Breyer et al.[79]
Power-to-hydrogen-to-power (PtH$_2$tP)	Technology Roadmap[80]	Jülch[4]
Power-to-methane-to-power (PtCH$_4$tP)	Technology Roadmap[80]	Jülch[4]

For today, three main conclusions can be drawn for the investigated basic ORC-based PTES systems (Figure 5-top): 1) The investigated ORC-based PTES systems are not economically competitive compared to PSH or CAES. PSH and CAES have a higher level of maturity today and are typically built with higher charge/discharge power ratings than PTES systems.[14] However, PSH and CAES are geographically limited; 2) The investigated ORC-based PTES systems are not economically competitive compared to PtH$_2$tP and PtCH$_4$tP technologies, which are, however, so far not established for large-scale electricity storage; and 3) Today, the SICs of the investigated ORC-based PTES systems are in the range of the SIC of Li-ion batteries (Li-ion), while PTES systems only require abundant materials, like steel, for their production. Furthermore, Li-ion batteries have a higher level of maturity today but are typically built with lower charge/discharge power ratings than PTES systems.[14]

Thus, as long as PtH$_2$tP and PtCH$_4$tP technologies are not established for large-scale electricity storage, the investigated basic ORC-based PTES system is an economical alternative electricity-storage technology with high-storage capacity for locations where PSH or CAES is not feasible.

For 2030 (Figure 5-bottom), the main conclusions for the investigated ORC-based PTES systems are as follows: 1) The SIC of CAES is expected to slightly increase until 2030 because an adiabatic CAES with additional heat storage is assumed to be state of the art.[4] The additional heat-storage increases efficiency and enables sector-coupling between the power and heat sectors. However, at the same time, the predicted SIC is slightly increased[4]; 2) The SIC of PtH$_2$tP technologies is expected to slightly decrease until 2030, while the SIC of PtCH$_4$tP technologies is expected to stay nearly constant; and 3) The SIC of Li-ion batteries is expected to significantly decrease in the next years. Thus, Li-ion batteries may become economically competitive to PtH2tP and PtCH4tP technologies, particularly considering the high efficiency of Li-ion batteries of up to 95%.[4]

ORC-based PTES systems may also become less expensive for several reasons: for example, the purchased-equipment cost of large-scale compressors could decrease, more advanced cycle configurations can be considered, or existing equipment of old, shutdown fossil power plants, particularly coal-fired power plants, can be used.[15] One reason to expect decreasing cost of large-scale compressors is that large-scale HPs are likely to become part of the future energy system.[83] In the future energy system, large-scale HPs can be a thermodynamically efficient alternative to carbon-intensive heating technologies, for example, fossil-fueled boilers. Thus, more large-scale compressor systems may be built in the future, increasing research and development activities in this field and reducing costs. In addition, all types of PTES systems are still in the development or research stage and thus they are expected to experience significant improvements in both efficiency and costs.[14]

Since the thermo-economic potential of ORC-based PTES systems has not been analyzed in detail in the literature, we compare our results with two economic studies investigating transcritical PTES systems: Morandin et al.[10] investigated complex cycle structures with up to 7 hot-storage tanks, a cold-storage cycle, and an optional additional ammonia cycle leading to specific purchased-equipment investment cost (SIC$_{PE}$) of 275–376 € kWh$_{out}^{-1}$. Henchoz et al.[66] analyzed a solar-enhanced PTES system with cold- and hot-storage cycles leading to SIC$_{PE}$ of 261 € kWh$_{out}^{-1}$. In these two studies, the SIC is significantly lower than the SIC for the investigated basic ORC-based PTES system. The main reason for the lower SIC is that solely the purchased-equipment cost is considered for the calculation and no additional correction factor is used to consider the cost for construction, piping, transport, control electronics, real estate, buildings, and planning (here: 3.4,[56] cf. Section 3.1). Considering solely the purchased-equipment cost and the compressor cost correlation from Henchoz et al.,[66] the thermo-economically optimal system for our case study leads to specific purchased-equipment investment cost of around 159 € kWh$_{out}^{-1}$. Thus, the presented 1-stage CoMT–CAMD method leads to a cost reduction of around 40% compared to similar transcritical PTES systems from the literature underlining the potential of the method.

Noteworthy, only the adiabatic CAES and the PTES systems can also be used to couple the heat and power sectors in the future. For example, waste heat can be directly stored in the thermal storage of the PTES or the heat can be used for heating applications. Consequently, PTES systems have a broad application range for heat and power. The broad application range and the possibility of sector coupling could make PTES systems a promising alternative large-scale storage technology in the future despite the comparatively high SIC.

5. Conclusion

In this work, we analyze the thermo-economic potential of a basic ORC-based PTES system by an integrated thermo-economic design of processes and working fluids. For this purpose, we successfully applied 1-stage CoMT–CAMD to design a basic PTES

system consisting of a large-scale HP, a thermal heat-storage cycle, and an ORC. Within the integrated design, we simultaneously optimize the HP, storage system, and ORC processes, and the working fluids of the HP and ORC. A consistent thermodynamic model is used to calculate both equilibrium and transport properties of the working fluids. Detailed models for sizing of the equipment are considered allowing for costing and thus considering a thermo-economic objective. The result of the integrated design is the optimal working fluid pair for HP and ORC and their corresponding optimal processes and equipment sizes for the HP, storage system, and ORC.

For the top five identified ORC-based PTES systems, C3 alkanes and alkenes are identified as promising working fluids for the ORC and C4 alkenes for the HP minimizing the SIC. The best working fluid pair is propane for the ORC and isobutene for the HP with $SIC = 929 \, \text{€} \, \text{kWh}_{out}^{-1}$ and a round-trip efficiency of $\eta = 36.7\%$. The optimal working fluid pair shows a good match of the temperature profiles between the sensible storage medium and the working fluids during condensation in the HP and evaporation in the ORC. Thereby, the exergy losses during heat transfer are reduced.

The largest cost contribution is due to the HP compressor. However, uncertainties in predicting the purchased-equipment cost of large-scale compressors are high due to lack of data. Two alternative cost correlations for the compressor change the SIC of the optimized PTES systems by -42% and $+31\%$. The result underlines the need for accurate cost correlations for large-scale compressors to refine the analysis and obtain more reliable results.

To quantify the economic potential of a basic ORC-based PTES system, we compared our results to alternative electricity-storage technologies. The comparison shows that the investigated basic ORC-based PTES system is not economically competitive to most state-of-the-art electricity storage technologies today. Solely Li-ion batteries have a similar cost range. In 2030, Li-ion batteries are expected to become significantly cheaper.

However, for ORC-based PTES systems, substantial cost reductions can also be expected in the future for several reasons: first, large-scale HPs are likely to become part of the future energy system, which could reduce the cost of large-scale compressors. Second, more advanced cycle configurations than the basic PTES could improve the efficiency of the PTES, for example, using cold or latent heat storage. Thus, an analysis of different flow sheets in a superstructure-based flow sheet design could identify less expensive systems, as shown for ORCs by Schilling et al.[49] Third, PTES systems have a broad application range with a high potential for sector coupling, for example, by storing waste heat or supplying a heat demand. Due to the expected high cost reduction potential, PTES systems could become economically competitive in the future.

Supporting Information

Supporting Information is available from the Wiley Online Library or from the author.

Conflict of Interest

The authors declare no conflict of interest.

Data Availability Statement

The data that support the findings of this study are available from the corresponding author upon reasonable request.

[1] M. Sterner, I. Stadler, *Energiespeicher - Bedarf, Technologien, Integration*, Springer, Berlin, Heidelberg **2017**.

[2] V. Wesselak, T. Schabbach, T. Link, J. Fischer, *Regenerative Energietechnik*, Springer, Berlin, Heidelberg **2013**.

[3] B. Swain, *Sep. Purif. Technol.* **2017**, *172*, 388.

[4] V. Jülch, *Appl. Energy* **2016**, *183*, 1594.

[5] A. Thess, *Phys. Rev. Lett.* **2013**, *111*, 110602.

[6] W.-D. Steinmann, *Renewable Sustainable Energy Rev.* **2017**, *75*, 205.

[7] T. Desrues, J. Ruer, P. Marty, J. F. Fourmigué, *Appl. Therm. Eng.* **2010**, *30*, 425.

[8] J. D. McTigue, A. J. White, C. N. Markides, *Appl. Energy* **2015**, *137*, 800.

[9] M. Mercangöz, J. Hemrle, L. Kaufmann, A. Z'Graggen, C. Ohler, *Energy* **2012**, *45*, 407.

[10] M. Morandin, M. Mercangöz, J. Hemrle, F. Maréchal, D. Favrat, *Energy* **2013**, *58*, 571.

[11] W. D. Steinmann, *Energy* **2014**, *69*, 543.

[12] G. F. Frate, M. Antonelli, U. Desideri, *Appl. Therm. Eng.* **2017**, *121*, 1051.

[13] W.-D. Steinmann, D. Bauer, H. Jockenhöfer, M. Johnson, *Energy* **2019**, *183*, 185.

[14] A. V. Olympios, J. D. McTigue, P. Farres-Antunez, A. Tafone, A. Romagnoli, Y. Li, Y. Ding, W.-D. Steinmann, L. Wang, *Energy* **2021**, *3*, 22001.

[15] W.-D. Steinmann, H. Jockenhöfer, D. Bauer, *Energy Technol.* **2020**, *8*, 1900895.

[16] Heaten AS, *HeatBooster - Very High Temperature Heat Pump* https://www.heaten.com/technology (accessed: February, 2022).

[17] S. Quoilin, M. van den Broek, S. Declaye, P. Dewallef, V. Lemort, *Renewable Sustainable Energy Rev.* **2013**, *22*, 168.

[18] D. Roskosch, B. Atakan, *Energy Procedia* **2017**, *129*, 1026.

[19] J. Koksharov, H. T. de Oliveira, F. Dammel, P. Stephan, *presented at 743. WE-Heraeus-Seminar*, March **2021**.

[20] A. I. Papadopoulos, I. Tsivintzelis, P. Linke, P. Seferlis, *Reference Module in Chemistry, Molecular Sciences and Chemical Engineering*, Elsevier **2018**, p. 1086 https://doi.org/10.1016/B978-0-12-409547-2.14342-2.

[21] R. Gani, *Comput. Chem. Eng.* **2004**, *28*, 2441.

[22] D. Roskosch, B. Atakan, *Energy* **2015**, *81*, 202.

[23] S. Cignitti, S. S. Mansouri, J. M. Woodley, J. Abildskov, *Ind. Eng. Chem. Res.* **2018**, *57*, 677.

[24] A. I. Papadopoulos, M. Stijepovic, P. Linke, *Appl. Therm. Eng.* **2010**, *30*, 760.

[25] M. Lampe, M. Stavrou, J. Schilling, E. Sauer, J. Gross, A. Bardow, *Comput. Chem. Eng.* **2015**, *81*, 278.

[26] J. Schilling, M. Lampe, J. Gross, A. Bardow, *Chem. Eng. Sci.* **2017**, *159*, 217.

[27] J. Schilling, D. Tillmanns, M. Lampe, M. Hopp, J. Gross, A. Bardow, *Mol. Syst. Des. Eng.* **2017**, *2*, 301.

[28] J. Frutiger, S. Cignitti, J. Abildskov, J. M. Woodley, G. Sin, *Comput. Chem. Eng.* **2019**, *122*, 247.

[29] S. Cignitti, J. G. Andreasen, F. Haglind, J. M. Woodley, J. Abildskov, *Appl. Energy* **2017**, *203*, 442.

[30] M. T. White, O. A. Oyewunmi, A. J. Haslam, C. N. Markides, *Energy Convers. Manage.* **2017**, *150*, 851.

[31] M. T. White, O. A. Oyewunmi, M. A. Chatzopoulou, A. M. Pantaleo, A. J. Haslam, C. N. Markides, *Energy* **2018**, *161*, 1181.

[32] L. M. T. van Kleef, O. A. Oyewunmi, C. N. Markides, *Appl. Energy* **2019**, *251*, 112513.

[33] J. Scheffczyk, L. Fleitmann, A. Schwarz, M. Lampe, A. Bardow, K. Leonhard, *Chem. Eng. Sci.* **2017**, *159*, 84.

[34] J. Scheffczyk, P. Schäfer, L. Fleitmann, J. Thien, C. Redepenning, K. Leonhard, W. Marquardt, A. Bardow, *Mol. Syst. Des. Eng.* **2018**, *3*, 645.

[35] J. Y. Ten, Z. H. Liew, X. Y. Oh, M. H. Hassim, N. Chemmangattuvalappil, *Process Integr. Optim. Sustainability* **2021**, *5*, 269.

[36] A. Bardow, K. Steur, J. Gross, *Ind. Eng. Chem. Res.* **2010**, *49*, 2834.

[37] M. Stavrou, M. Lampe, A. Bardow, J. Gross, *Ind. Eng. Chem. Res.* **2014**, *53*, 18029.

[38] F. E. Pereira, E. Keskes, A. Galindo, G. Jackson, C. S. Adjiman, *Process Systems Engineering*, Wiley-VCH, Weinheim, Germany **2008**, pp. 231–248.

[39] F. E. Pereira, E. Keskes, A. Galindo, G. Jackson, C. S. Adjiman, *Comput. Chem. Eng.* **2011**, *35*, 474.

[40] J. Burger, V. Papaioannou, S. Gopinath, G. Jackson, A. Galindo, C. S. Adjiman, *AIChE J.* **2015**, *61*, 3249.

[41] S. Gopinath, G. Jackson, A. Galindo, C. S. Adjiman, *AIChE J.* **2016**, *62*, 3484.

[42] T. Zhou, Y. Zhou, K. Sundmacher, *Chem. Eng. Sci.* **2017**, *159*, 207.

[43] T. Zhou, K. McBride, X. Zhang, Z. Qi, K. Sundmacher, *AIChE J.* **2015**, *61*, 147.

[44] C. Gertig, L. Fleitmann, J. Schilling, K. Leonhard, A. Bardow, *Chem. Ing. Tech.* **2020**, *92*, 1489.

[45] C. Gertig, K. Leonhard, A. Bardow, *Curr. Opin. Chem. Eng.* **2020**, *27*, 89.

[46] J. Gross, G. Sadowski, *Ind. Eng. Chem. Res.* **2001**, *40*, 1244.

[47] M. Morandin, F. Maréchal, M. Mercangöz, F. Buchter, *Energy* **2012**, *45*, 375.

[48] S. Lecompte, H. Huisseune, M. van den Broek, B. Vanslambrouck, M. de Paepe, *Renewable Sustainable Energy Rev.* **2015**, *47*, 448.

[49] J. Schilling, C. Horend, A. Bardow, *AIChE J.* **2020**, *66*, e16903.

[50] H. Struebing, *Dissertation*, Imperial College London **2011**.

[51] H. Struebing, *Optimal Solvent Design for Reactions using Computer-Aided Molecular Design*, http://www.minlp.org/library/problem/mod/index.php?lib=MINLP&i=180&pi=-137, (accessed: February, 2022).

[52] J. Schilling, *Dissertation*, RWTH Aachen University **2020**.

[53] Process Systems Enterprise, gPROMS, https://www.psenterprise.com/products/gproms, (accessed: February, 2022).

[54] M. A. Duran, I. E. Grossmann, *Math. Program.* **1986**, *36*, 307.

[55] I. E. Grossmann, Z. Kravanja, *Comput. Chem. Eng.* **1995**, *19*, 189.

[56] R. Smith, *Chemical Process Design and Integration*, Wiley, Chichester, West Sussex **2005**.

[57] M. Astolfi, M. C. Romano, P. Bombarda, E. Macchi, *Energy* **2014**, *66*, 435.

[58] R. Turton, *Analysis, Synthesis, and Design of Chemical Processes*, Prentice Hall, Upper Saddle River, NJ **2012**.

[59] G. Towler, R. Sinnott in *Chemical Engineering Design*, Elsevier **2013**, pp. 307–354.

[60] V. Gnielinski, *NASA STI/Recon. Tech. Rep. A* **1975**, *41*, 8.

[61] K. E. Gungor, R. H. S. Winterton, *Int. J. Heat Mass Transfer* **1986**, *29*, 351.

[62] R. Numrich, J. Müller in *VDI Heat Atlas*, Springer, Berlin, Heidelberg **2010**, pp. 903–918.

[63] DIN EN 13455-3, *Unfired Pressure Vessels - Part 3: Design; German Version EN 13445-3:2014/A6:2019*, **2019**.

[64] EN 14015:2004, *Specification for the design and manufacture of site built, vertical, cylindrical, flat-bottomed, above ground, welded, steel tanks for the storage of liquids at ambient temperature and above; German version EN 14015:2004*, **2005**.

[65] R. Jacob, W. Saman, F. Bruno, *AIP Conf. Proc.* **2017**, *1850*, 080012.

[66] S. Henchoz, F. Buchter, D. Favrat, M. Morandin, M. Mercangöz, *Energy* **2012**, *45*, 358.

[67] E. Sauer, M. Stavrou, J. Gross, *Ind. Eng. Chem. Res.* **2014**, *53*, 14854.

[68] J. Vijande, M. M. Piñeiro, D. Bessières, H. Saint-Guirons, J. L. Legido, *Phys. Chem. Chem. Phys.* **2004**, *6*, 766.

[69] K. G. Joback, R. C. Reid, *Chem. Eng. Commun.* **1987**, *57*, 233.

[70] O. Lötgering-Lin, J. Gross, *Ind. Eng. Chem. Res.* **2015**, *54*, 7942.

[71] M. Hopp, J. Gross, *Ind. Eng. Chem. Res.* **2019**, *58*, 20441.

[72] Y. Rosenfeld, *Phys. Rev. A* **1977**, *15*, 2545.

[73] Y. Rosenfeld, *J. Phys.: Condens. Matter* **1999**, *11*, 5415.

[74] J. Gross, *AIChE J.* **2005**, *51*, 2556.

[75] J. Gross, J. Vrabec, *AIChE J.* **2006**, *52*, 1194.

[76] C. Yue, D. Han, W. Pu, W. He, *Renewable Energy* **2015**, *80*, 746.

[77] J. B. Jensen, S. Skogestad, *Computer Aided Chemical Engineering*, Elsevier **2005**, pp. 1429–1434 https://doi.org/10.1016/S1570-7946(05)80080-X.

[78] *Product and Process Design Principles: Synthesis, Analysis and Evaluation - 4th Edition*, (Eds: W. D. Seider, D. R. Lewin, J. D. Seader, S. Widagdo, R. Gani, K. M. Ng), Wiley, New York **2016**.

[79] C. Breyer, D. Bogdanov, A. Aghahosseini, A. Gulagi, M. Child, A. S. Oyewo, J. Farfan, K. Sadovskaia, P. Vainikka, *Prog. Photovoltaics Res. Appl.* **2018**, *26*, 505.

[80] IEA, *Technology Roadmap - Hydrogen and Fuel Cells*, IEA, Paris **2015**.

[81] R. Haas, C. Kemfert, H. Auer, A. Ajanovic, M. Sayer, A. Hiesl, *WIREs Energy Environ.* **2022**, *8*, e318.

[82] S. Lecompte, S. Lemmens, H. Huisseune, M. van der Broek, M. de Paepe, *Energies* **2015**, *8*, 2714.

[83] F. Schlosser, M. Jesper, J. Vogelsang, T. G. Walmsley, C. Arpagaus, J. Hesselbach, *Renewable Sustainable Energy Rev.* **2020**, *133*, 110219.